JOURNAL OF MATERIALS SCIENCE 28 (1993) 1983–1987

Interfacial reactions in a Ti–6Al–4V based composite: role of the TiB_2 coating

M. FERRARIS*
Centro Ricerche Fiat, St. Torino 50, I 10043 Orbassano (To), Italy

C. BADINI, F. MARINO
Dipartimento di Scienza dei Materiali e Ingegneria Chimica, Politecnico di Torino, C. so Duca degli Abruzzi 24, I 10129 Torino, Italy

F. MARCHETTI, S. GIRARDI
IRST, Divisione Scienza dei Materiali, Loc. Pantè di Povo, I 38100 Trento, Italy

The characterization of TiB_2/C-coated SiC fibres and their interface region in a Ti–6Al–4V based composite has been performed by using scanning electron microscopy (SEM), energy-dispersion X-rays (EDX) and Auger electron spectroscopy (AES). The features of the as-received fibre and the reactivity between fibre and matrix occurring during preparation of the composite have been studied in this paper. The interaction of the TiB_2 external coating of the fibre with both the adjacent carbon layer and the titanium-based matrix is already appreciable in the as-received composite: TiB needles grow from TiB_2 towards the matrix and a new layer containing C, Ti and B appears between TiB_2 and C. The thicknesses of the original carbon and TiB_2 fibre coatings decrease in the composite from 1000 nm to 400 and 800 nm, respectively. The TiB_2 inhibits the reaction between SiC and Ti: there is no evidence of Si_xTi_y brittle phases.

1. Introduction

Titanium-matrix composites reinforced with long fibres are of great technological importance because of their application as structural components (aerospace industry, gas turbines etc.) [1]. Several kinds of fibres have been used: B, B_4C-coated B, SiC fibre with C or W core [2–6]. Because of the reactivity of Ti matrix with these fibres, particular coatings have been developed: SCS-6 (Avco) [7, 8] has been especially designed for mechanical protection of the fibre and for inhibiting detrimental reactions between SiC and Ti. This fibre coating, mainly consisting of carbon with small amounts of dispersed SiC and an outer layer richer in SiC, has been tailored to avoid direct reaction between the matrix and the fibre during preparation of the composite. Actually, the coating partially reacts with the matrix giving brittle phases which decrease the mechanical strength of the composite.

A new coating for SiC fibres reinforcing a Ti matrix has been developed by BP Metal Composites Ltd: it consists of an internal carbon layer and an external one of TiB_2, both about 1 μm thick. Preliminary data on the morphology and composition of this protective coating and its modification during isothermal treatment were previously reported [9]. The preparation of the composite follows the standard hot-pressing technique [10].

The aim of this paper is the microstructural characterization of the C/TiB_2 coating before and after preparation of the composite.

2. Experimental procedure

The titanium-based composite and the single filament were supplied by BP Metal Composites Ltd: the fibre is a TiB_2/C-coated SiC monofilament with a tungsten core and the matrix is a Ti–6Al–4V alloy. The six-ply unidirectional panels were prepared according to usual vacuum hot-pressing techniques, with 75 μm foils and fibre mats. The fibres were hot-pressed between the matrix foils at about 900 °C, 90–180 MPa for 20–30 min [11]. The as-received material was cut perpendicularly to the fibre direction with a low-speed diamond saw, then polished and etched on the cross-section.

The TiB_2/C-coated SiC fibre was carefully handled and resin-embedded to avoid cracks between the two layers of the coating. In spite of that, some fibre cross-sections showed failures between the two layers. The diameters of the fibre and the tungsten core are about 100 and 12 μm respectively.

The fibre–matrix interaction zone was studied by scanning electron microscopy (SEM) (Philips 525 M), energy-dispersive X-ray analysis (EDX) (Philips EDAX 9100), Auger electron spectroscopy (AES) (Thin Film Analyser–Physical Electronics Model 4200).

The Auger analyses were carried out in a chamber with a base pressure of 10^{-10} torr using a cylindrical mirror analyser (CMA) with energy resolution of 0.6%. The primary electron beam, generated by an electron gun coaxial with the CMA, operates at 5 keV

0022–2461

in scanning mode (10^{-3} mm^2 irradiated area). The beam diameter is estimated to be about 4 μm. Data were acquired in integral mode (voltage to frequency converter) and in order to measure the signal intensities, spectra were computer-differentiated.

Sputtering was accomplished with a differentially pumped ion gun (PHI Model 04-300) generating an Ar^+ ion beam at 4 keV. The angle between the normal to the sample surface and the ion beam was fixed at 50° and an area of 1 mm^2 was rastered by the ion beam.

Depth profiles were carried out by alternating sputtering and Auger acquisition. Analyses were performed in the centre of the ion-beam irradiated area in order to avoid possible crater effects. Samples were angle-polished at about 5° from the fibre axis (without etching the sample).

In order to simulate the reactions occurring in one interfacial zone, titanium diboride and graphite powders were mixed, cold-pressed, vacuum-sealed in a pure silica tube and heated at different temperatures ranging between 850 and 1000 °C for 30 min up to 20 days. A reaction time much longer than for the composite process was necessary to approach thermodynamical equilibrium between C and TiB_2.

XRD spectra (CuK_α radiation) of the powders were recorded in the range of $\theta = 10$–$35°$ using a Philips PW1710.

3. Results

Fig. 1 shows the cross-section of an as-received fibre with the two layers (about 1000 nm thick). EDX and AES analyses performed on the fibre revealed the presence of titanium and boron in the external layer, carbon in the internal one, and silicon and carbon inside the fibre.

Fig. 2 shows the typical fibre–matrix reaction zone for the as-received composite: the main morphological feature observed is the presence of three layers, labelled 1, 2, 3 in the micrograph. The thickness of layers 1 and 2 is less than 1000 nm (about 400 nm). Sharp needles (bright in the SEM micrograph) grow from layer 3 toward the matrix.

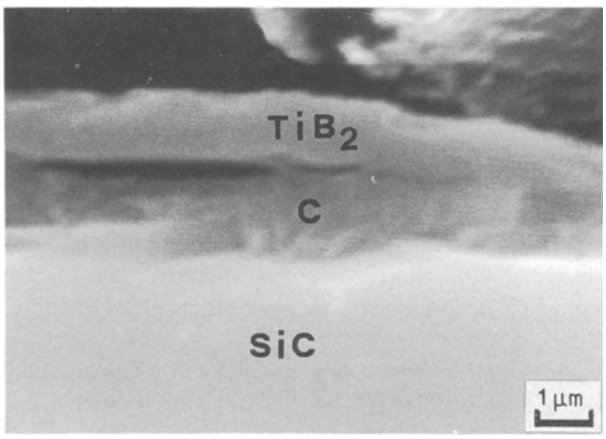

Figure 1 TiB_2/C-coated SiC fibre (resin embedded); SEM micrograph.

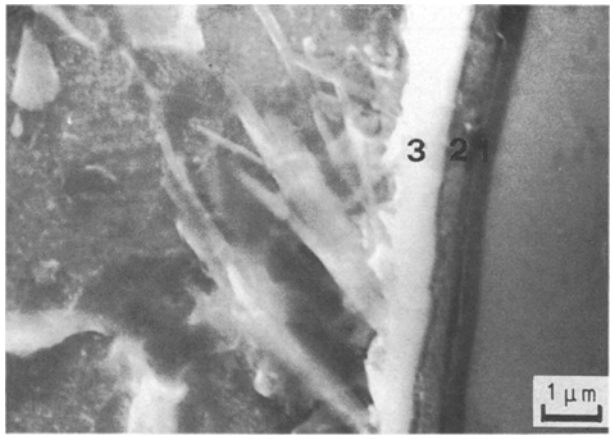

Figure 2 As-received composite: fibre–matrix interaction zone; SEM micrograph.

As the three layers are very thin, a technique like energy-dispersive X-ray analysis does not have enough spatial resolution and gives averaged compositional values (e.g. 1.7 μm spatial resolution at 10 keV for TiB_2). Other techniques like transmission electron microscopy and X-ray mapping have been used [12] to characterize the interface in this composite.

In order to obtain a complete characterization of the chemical composition of this system, in particular for the fibre–matrix reaction zones, Auger depth profiles were performed. The sputtering removes the materials with a resolution of a few tenths of a nanometre: the depth resolution is associated with the Auger signal, which is directly connected to the energy of specific Auger electrons [13]. Another important advantage related to AES is the possibility of obtaining chemical information by studying the line-shape of the Auger transitions that involve electrons of the valence band [14].

Fig. 3 shows the typical Auger depth profile obtained for the interface region shown in Fig. 2. In order to avoid misunderstandings due to particular features of the interface like topographic defects, sputtering artefacts etc., several depth profiles were recorded with the same experimental conditions, at different points. The same profile as that shown in Fig. 3 was obtained in all cases. The peak-to-peak height ratios of each signal, obtained from the derivative spectrum, were normalized to the maximum value measured on the depth profile.

Looking in more detail at the behaviour of the different signals and, when possible, the Auger lineshape, several zones have been singled out in the depth profile of Fig. 3. In particular five zones (labelled a, b, c, d, e) show the different features described below.

Zone a. The region between 0 and 70 min of sputtering is characterized by a constant titanium intensity. Vanadium and aluminium signals, which follow in this region the same behaviour as titanium, are not represented because of their low intensity. No other signals are present. The spectrum here is typical of the Ti–6Al–4V bulk matrix.

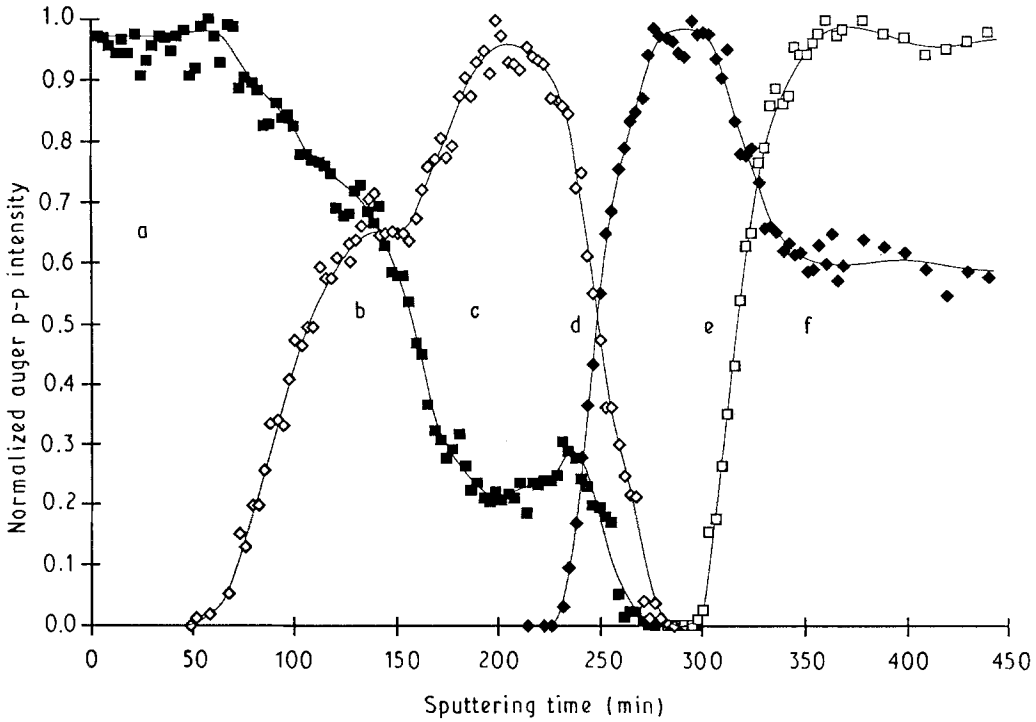

Figure 3 AES depth-profile of the fibre–matrix interaction zone: (■) Ti, (□) Si, (◇) B, (◆) C. For further explanation see text.

Zone b. In the region from 70 to 150 min of sputtering the titanium signal shows a more or less gradual decrease up to an intensity about 70% of the bulk value, whereas the boron signal increases. This zone is representative of a non-homogeneous layer (TiB + matrix), both from a morphological and compositional point of view.

Zone c. The region from 150 to 215 min of sputtering is again characterized by the presence of only boron and titanium signals. After a steeper decrease (if compared with the previous one) titanium reaches a plateau in which the Auger intensity is about 20% of the matrix value; at the same time the boron signal reaches a plateau value that represents the maximum intensity of this element in the depth profile. The Auger line-shape of boron *KVV* in this region is very similar to those of other transition metal borides [15]. Furthermore, this line-shape is in very good agreement with those acquired, in our laboratory, on a standard sample of TiB_2.

Zone d. From 215 to 270 min of sputtering, while the boron signal progressively decreases and disappears, the titanium signal shows a non-monotonic behaviour with first a weak increase and then a decrease to zero. Another important aspect of this region is the presence of the carbon signal, which shows an increasing trend. It must be emphasized that this is the only zone with three detectable elements.

Zone e. In the region from 270 to 310 min of sputtering the only detectable element is carbon. Its Auger signal reaches the maximum value and its lineshape (C *KVV*) is typical of carbon in graphitic form [16].

Zone f. In the last region, from 310 min of sputtering to the end of the profile, there are only carbon and silicon signals. Their intensities reach a constant value in function of the sputtering time. The line-shapes of their Auger spectra (C *KVV* and Si *L2*, *3VV*) are typical of silicon carbide [17].

To summarize, the AES depth profile of Fig. 3 shows well-defined regions: (a) Ti–6Al–4V matrix, (b) TiB + matrix, (c) TiB_2, (d) reaction zone of Ti + B + C, (e) graphite and (f) silicon carbide. As can be seen by comparison of Figs 2 and 3, good agreement exists between the morphology and the picture of the sample obtained from the Auger depth profile. Hence, it is possible to obtain a translation of the sputtering time scale to a thickness scale, adding the following hypothesis: that the sputtering rate along the profile is constant and material-independent. The zones e, d and c of Fig. 3 defined above as graphite, C + B + Ti and TiB_2 correspond to 40, 55 and 65 min of sputtering, respectively; the layers labelled 1, 2 and 3 in Fig. 2 are of thickness 400, 400 and 800 nm, respectively.

XRD analyses of TiB_2 and C powder mixtures heated at 850–1000 °C for different times (up to 20 days) have shown neither the formation of carbides/borocarbides, nor any appreciable variation of TiB_2 lattice parameters, but a remarkable decrease of the carbon peak intensity.

4. Discussion

Some interactions between the fibre coatings and the Ti–6Al–4V occur during preparation of the composite, and in particular these have been observed at the matrix–TiB_2 and TiB_2–C interfaces.

The TiB_2 layer slightly reduces in thickness (compare the external layer in Figs 1 and 2); as Fig. 2 shows, it is surrounded by bright needles, identified as TiB from several authors in composites like Ti–6Al–4V/B and Ti–6Al–4V/B(B_4C) [3, 18–23].

It is clear from AES profiles (Fig. 3) that Ti slowly decreases from the value of the matrix towards lower values attributable to the presence of TiB (zone b) and TiB_2 (zone c), while B slowly increases its concentration in the same regions. That means that TiB_2 reacts with the matrix during the preparation of the composite according to the equation

$$TiB_2 + Ti \rightarrow 2TiB$$

A zone of interaction with C, Ti and B is immediately noticeable between the layers of TiB_2 and C (Fig. 3d). An intermediate zone is visible in the micrograph (Fig. 2), with a lighter grey compared to the adjacent carbon layer. The Ti–C–B phase diagram is not completely known; only the reactions occurring between TiB_2 and C or TiB and B_4C have been reported [24].

TiB_2 seems to be very stable with respect to TiB. In fact, while TiB can react with C to form Ti(B, C) [20], reactions between TiB_2 and C were not reported. A sort of simulation of this solid-state reaction has been attempted by heating TiB_2 and C as described above: TiB_2 did not appreciably change its lattice parameters, but the intensity of C peaks decreased remarkably in the X-ray patterns. On the other hand, TiB_2 does not have a definite stoichiometry, but a compositional range of 65.5–66.7 at% B [24]. The existence of $Ti(B, C)_2$ solid solutions should be proposed; furthermore, the covalent radii of B and C are similar (82 and 77×10^{-12} m, respectively). It is also to be taken in account that the high concentration of vacancies in chemical vapour-deposited TiB_2 and C coatings of the fibres increases the possibility for the formation of solid solution.

However, the experiment described above shows that no reactions occurred between TiB_2 and C. Nevertheless, about a half of the carbon layer undergoes a modification (Fig. 2) and a maximum for the titanium concentration in zone d of AES profile (Fig. 3) is observed. Hence, in order to explain the feature of zone d another reaction must be inferred: after diffusion from the matrix through the TiB_2 layer, Ti reacts with TiB_2 and C giving the Ti(B, C) phase.

The carbon concentration grows through the region described above (d) to a zone of maximum (e). No other elements have been detected in this zone, which corresponds to the graphitic carbon layer originally deposited on the SiC fibre. After the graphitic layer there is finally the SiC fibre with Si and C at constant atomic percentage.

The silicon profile is well separated from the Ti and B ones: this is remarkable as it means that no interactions have occurred between Si and Ti. That means that the brittle phase Ti_xSi_y does not grow [1–3, 5, 6, 8]. As a consequence, this composite shows good mechanical properties: a strength greater than 1700 MPa and a stiffness of 210 GPa [10].

To summarize, the thin TiB_2 layer (originally 1 μm) acts as an effective barrier for the diffusion of Ti. As a consequence, it slows down the movement of titanium atoms towards the more internal layer of carbon and the SiC fibre. Only after diffusion of titanium through TiB_2, can Ti react with the carbon to form carbides or boroncarbides.

However, the double TiB_2/C protection for the SiC fibre involves a different mechanism with respect to that observed for SCS fibres [7, 8]. In the case of SCS fibres the double carbon/carbon–SiC layer is basically a sacrificial coating which reacts with the matrix. Due to this reaction Ti_5Si_3 and TiC (1.5 μm thick) form at the interface with the matrix during the preparation of SCS-reinforced composites. These brittle layers affect the mechanical behaviour of the composites, as the fracture takes place at the interface between TiC and the more internal layer of C [8].

In contrast, in the case of TiB_2/C double-coated SiC fibres, the formation of a brittle phase containing Ti and C needs the previous diffusion of titanium through the TiB_2 layer. On the other hand, brittle TiB crystals easily form by reaction of TiB_2 with titanium alloy during the processing of the composite.

5. Conclusions

1. The C/TiB_2 coating is an effective protection for SiC fibres from detrimental reactions with Ti matrix.
2. There is no evidence for the formation of a brittle Si_xTi_y phase: Si and Ti AES profiles are well separated.
3. TiB_2 reacts with the Ti matrix giving TiB needles.
4. TiB_2 also reacts with the diffused Ti and C giving a Ti–B–C interphase.

Acknowledgements

The authors wish to thank Professor P. Appendino for helpful discussions and BP Metal Composites Ltd. for supplying the fibres; one of us (M.F.) also thanks Mr DiTollo and Mr Messina (Centro Ricerche Fiat) for their help with SEM and the CRF Director for permission to publish this paper.

References

1. P. R. SMITH and F. H. FROES, *J. Metals* **36** (1984) 19.
2. E. P. ZIRONI and H. POPPA, *J. Mater. Sci.* **16** (1981) 3115.
3. R. PAILLER, P. MARTINEAU, M. LAHAYE and R. NASLAIN, *Rev. Chimie Min.* **18** (1981) 520.
4. P. MARTINEAU, M. LAHAYE, R. PAILLER, R. NASLAIN, M. COUZI and F. CREUGE, *J. Mater. Sci.* **19** (1984) 2731.
5. P. MARTINEAU, M. LAHAYE, R. PAILLER and R. NASLAIN, *ibid.* **19** (1984) 2749.
6. T. CHRISTMAN, K. HEADY and T. VREELAND Jr, *Scripta Metall.* **25** (1991) 631.
7. C. JONES, C. J. KIELY and S. S. WANG, *J. Mater. Res.* **5** (1990) 1435.
8. *Idem, ibid.* **4** (1989) 327.
9. P. APPENDINO, C. BADINI, M. FERRARIS, F. MARINO and M. MONTORSI, in Proceedings, 13° Conv. Naz. Trattamenti Termici, Salsomaggiore, Italy, November 1991 (Associazione Italiana di Metallurgia, Milano, 1991) p. 25.
10. N. A. JAMES, D. V. LOVETT and C. M. WARWICK, in Proceedings of International Conference on Composite Materials (ICCM/8), Honolulu, July 1991, paper 19-I. Edited by S. W. Tsai and G. S. Springer. Stanford University, USA.
11. A. TARRANT, BP Metal Composites (UK), Private Communication, 1992.
12. B. DERBY, (Department of Materials, Oxford University, UK) Private Communication, 1992.
13. P. SEAH and W. A. DENCH, *Surf. Interf. Anal.* **1** (1979) 2.
14. R. WEISSMANN and K. MULLER, *Surf. Sci. Rep.* **105** (1981) 251.
15. L. GONZO, L. CALLIARI and F. MARCHETTI, *Vuoto* **20** (1990) 341.

16. D. E. RAMAKER, *Appl. Surf. Sci.* **21** (1985) 243.
17. F. BOZSO, L. MUELHOFF, M. TRENARY, W. J. CHOYCKE and J. T. YATES Jr, *J. Vac. Sci. Technol.* **A2** (1984) 1271.
18. V. A. NERONOV, M. A. KORCHAGIN, V. V. ALEKSANDROV and S. N. GUSENKO, *J. Less-Common Met.* **82** (1981) 125.
19. P. R. SMITH, F. H. FROES and J. T. CAMMETT, in Proceedings of Conference on Mechanical Behaviour of Metal Matrix Composites, Dallas, February 1982, p. 143. The Metallurgical Society, AIME, USA.
20. J. THEBAULT, R. PAILLER, G. BONTEMPS-MOLEY, M. BOURDEAU and R. NASLAIN, *J. Less-Common Met.* **47** (1976) 221.
21. P. SOUMELIDIS, J. M. QUENISSET, R. NASLAIN and N. S. STOLOFF, *J. Mater. Sci.* **21** (1986) 895.
22. G. METCALFE and M. J. KLEIN, in Proceedings of 2nd International Conference of the Metallurgical Society of AIME, Cambridge, USA, May 1972, p. 2285. Edited by R. I. Jaffee and H. M. Burte, Plenum Press, 1973.
23. J. W. STEEDS and C. G. RHODES, *J. Amer. Ceram. Soc.* **68** (1985) C-136.
24. F. W. GLASER, *J. Metals* **4** (1952) 391.

Received 28 July
and accepted 11 August 1992